

Encoding multiple holograms for speckle-noise reduction in optical display

Pasquale Memmolo,^{1,2,*} Vittorio Bianco,¹ Melania Paturzo,¹ Bahram Javidi,³ Paolo A. Netti,² and Pietro Ferraro¹

¹CNR-Istituto Nazionale di Ottica, via Campi Flegrei 34, 80078 Pozzuoli (NA), Italy

²Center for Advanced Biomaterials for HealthCare@CRIB, Istituto Italiano di tecnologia, Largo Barsanti e Matteucci 53, 80125 Napoli, Italy

³ECE Department, University of Connecticut, U-157, Storrs, Connecticut 06269, USA

*pasquale.memmolo@ino.it

Abstract: In digital holography (DH) a mixture of speckle and incoherent additive noise, which appears in numerical as well as in optical reconstruction, typically degrades the information of the object wavefront. Several methods have been proposed in order to suppress the noise contributions during recording or even during the reconstruction steps. Many of them are based on the incoherent combination of multiple holographic reconstructions achieving remarkable improvement, but only in the numerical reconstruction i.e. visualization on a pc monitor. So far, it has not been shown the direct synthesis of a digital hologram which provides the denoised optical reconstruction. Here, we propose a new effective method for encoding in a single complex wavefront the contribution of multiple incoherent reconstructions, thus allowing to obtain a single synthetic digital hologram that show significant speckle-reduction when optically projected by a Spatial Light Modulator (SLM).

©2014 Optical Society of America

OCIS codes: (090.1995) Digital holography; (090.4220) Multiplex holography; (090.2870) Holographic display; (100.3010) Image reconstruction techniques.

References and links

1. W. Osten and P. Ferraro, Digital holography and its application in MEMS/MOEMS inspection,” in “Optical Inspection of Microsystems,” in vol. **109** of *Optical Science and Engineering Series*, W. Osten ed. (CRC Press), 351–425 (2006).
2. P. Ferraro, A. Wax, and Z. Zalevsky, eds., “Coherent light microscopy,” in *Springer Series in Surface Sciences*, vol. **46** (Springer, 2011).
3. P. Memmolo, V. Bianco, F. Merola, L. Miccio, M. Paturzo, and P. Ferraro, “Breakthroughs in Photonics 2013: Holographic Imaging,” *IEEE Photonics Journal* **6**(2), 701106 (2014).
4. F. Merola, L. Miccio, P. Memmolo, G. Di Caprio, A. Galli, R. Puglisi, D. Balduzzi, G. Coppola, P. Netti, and P. Ferraro, “Digital holography as a method for 3D imaging and estimating the biovolume of motile cells,” *Lab Chip* **13**(23), 4512–4516 (2013).
5. L. Miccio, P. Memmolo, F. Merola, S. Fusco, V. Embrione, A. Paciello, M. Ventre, P. A. Netti, and P. Ferraro, “Particle tracking by full-field complex wavefront subtraction in digital holography microscopy,” *Lab Chip* **14**(6), 1129–1134 (2014).
6. M. Paturzo, P. Memmolo, A. Finizio, R. Näsänen, T. J. Naughton, and P. Ferraro, “Synthesis and display of dynamic holographic 3D scenes with real-world objects,” *Opt. Express* **18**(9), 8806–8815 (2010).
7. M. Locatelli, E. Pugliese, M. Paturzo, V. Bianco, A. Finizio, A. Pelagotti, P. Poggi, L. Miccio, R. Meucci, and P. Ferraro, “Imaging live humans through smoke and flames using far-infrared digital holography,” *Opt. Express* **21**(5), 5379–5390 (2013).
8. S. Fukushima, T. Kurokawa, and M. Ohno, “Real-time hologram construction and reconstruction using a high resolution spatial light-modulator,” *Appl. Phys. Lett.* **58**(8), 787–789 (1991).
9. E. Stoykova, F. Yaraş, H. Kang, L. Onural, A. Geltrude, M. Locatelli, M. Paturzo, A. Pelagotti, R. Meucci, and P. Ferraro, “Visible reconstruction by a circular holographic display from digital holograms recorded under infrared illumination,” *Opt. Lett.* **37**(15), 3120–3122 (2012).
10. T. Shimobaba, M. Makowski, T. Kakue, M. Oikawa, N. Okada, Y. Endo, R. Hirayama, and T. Ito, “Lensless zoomable holographic projection using scaled Fresnel diffraction,” *Opt. Express* **21**(21), 25285–25290 (2013).

11. M. Kujawinska, T. Kozacki, C. Falldorf, T. Meeser, B. M. Hennelly, P. Garbat, W. Zaperty, M. Niemelä, G. Finke, M. Kowiel, and T. Naughton, "Multiwavefront digital holographic television," *Opt. Express* **22**(3), 2324–2336 (2014).
12. S. Soththivirat and J. A. Fessler, "Penalized-likelihood image reconstruction for digital holography," *J. Opt. Soc. Am. A* **21**(5), 737–750 (2004).
13. D. Cojoc, S. Finaurini, P. Livshits, E. Gur, A. Shapira, V. Mico, and Z. Zalevsky, "Toward fast malaria detection by secondary speckle sensing microscopy," *Biomed. Opt. Express* **3**(5), 991–1005 (2012).
14. A. Uzan, Y. Rivenson, and A. Stern, "Speckle denoising in digital holography by nonlocal means filtering," *Appl. Opt.* **52**(1), A195–A200 (2013).
15. J. Maycock, B. M. Hennelly, J. B. McDonald, Y. Frauel, A. Castro, B. Javidi, and T. J. Naughton, "Reduction of speckle in digital holography by discrete Fourier filtering," *J. Opt. Soc. Am. A* **24**(6), 1617–1622 (2007).
16. J. G. Sucerquia, J. A. H. Ramirez, and D. V. Prieto, "Reduction of speckle noise in digital holography by using digital image processing," *Optik (Stuttg.)* **116**(1), 44–48 (2005).
17. P. Memmolo, I. Esnaola, A. Finizio, M. Paturzo, P. Ferraro, and A. M. Tulino, "SPADEDH: a sparsity-based denoising method of digital holograms without knowing the noise statistics," *Opt. Express* **20**(15), 17250–17257 (2012).
18. M. Abollashani and Y. Rostami, "Speckle noise reduction by division and digital processing of a hologram," *Optik (Stuttg.)* **123**(10), 937–939 (2012).
19. B. Redding, M. A. Choma, and H. Cao, "Speckle-free laser imaging using random laser illumination," *Nat. Photonics* **6**(6), 355–359 (2012).
20. J. Garcia-Sucerquia, "Noise reduction in digital lensless holographic microscopy by engineering the light from a light-emitting diode," *Appl. Opt.* **52**(1), A232–A239 (2013).
21. Y. Wang, P. Meng, D. Wang, L. Rong, and S. Panezai, "Speckle noise suppression in digital holography by angular diversity with phase-only spatial light modulator," *Opt. Express* **21**(17), 19568–19578 (2013).
22. A. Jesacher, C. Maurer, A. Schwaighofer, S. Bernet, and M. Ritsch-Marte, "Near-perfect hologram reconstruction with a spatial light modulator," *Opt. Express* **16**(4), 2597–2603 (2008).
23. Y. Kuratomi, K. Sekiya, H. Satoh, T. Tomiyama, T. Kawakami, B. Katagiri, Y. Suzuki, and T. Uchida, "Speckle reduction mechanism in laser rear projection displays using a small moving diffuser," *J. Opt. Soc. Am. A* **27**(8), 1812–1817 (2010).
24. S. Kubota and J. W. Goodman, "Very efficient speckle contrast reduction realized by moving diffuser device," *Appl. Opt.* **49**(23), 4385–4391 (2010).
25. F. Pan, W. Xiao, S. Liu, F. Wang, L. Rong, and R. Li, "Coherent noise reduction in digital holographic phase contrast microscopy by slightly shifting object," *Opt. Express* **19**(5), 3862–3869 (2011).
26. T. Baumbach, E. Kolenovic, V. Kebbel, and W. Jüptner, "Improvement of accuracy in digital holography by use of multiple holograms," *Appl. Opt.* **45**(24), 6077–6085 (2006).
27. C. G. Quan, X. Kang, and C. J. Tay, "Speckle noise reduction in digital holography by multiple holograms," *Opt. Eng.* **46**(11), 115801 (2007).
28. M. Leo, C. Distante, M. Paturzo, P. Memmolo, M. Locatelli, E. Pugliese, R. Meucci, and P. Ferraro, "Automatic digital hologram denoising by spatiotemporal analysis of pixel-wise statistics," *J. Display Technol.* **9**(11), 904–909 (2013).
29. L. Rong, W. Xiao, F. Pan, S. Liu, and R. Li, "Speckle noise reduction in digital holography by use of multiple polarization holograms," *Chin. Opt. Lett.* **8**(7), 653–655 (2010).
30. H. Jiang, J. Zhao, and J. Di, "Digital color holographic recording and reconstruction using synthetic aperture and multiple reference waves," *Opt. Commun.* **285**(13–14), 3046–3049 (2012).
31. V. Bianco, M. Paturzo, A. Finizio, D. Balduzzi, R. Puglisi, A. Galli, and P. Ferraro, "Clear coherent imaging in turbid microfluidics by multiple holographic acquisitions," *Opt. Lett.* **37**(20), 4212–4214 (2012).
32. V. Bianco, M. Paturzo, O. Gennari, A. Finizio, and P. Ferraro, "Imaging through scattering microfluidic channels by digital holography for information recovery in lab on chip," *Opt. Express* **21**(20), 23985–23996 (2013).
33. V. Bianco, M. Paturzo, A. Finizio, A. Calabuig, B. Javidi, and P. Ferraro, "Clear microfluidics imaging through flowing blood by digital holography," *IEEE J. Sel. Top. Quantum Electron.* **20**(3), 6801507 (2014).
34. Y. S. Kim, T. Kim, S. S. Woo, H. Kang, T. C. Poon, and C. Zhou, "Speckle-free digital holographic recording of a diffusely reflecting object," *Opt. Express* **21**(7), 8183–8189 (2013).
35. N. Bertaux, Y. Frauel, P. Réfrégier, and B. Javidi, "Speckle removal using a maximum-likelihood technique with isoline gray-level regularization," *J. Opt. Soc. Am. A* **21**(12), 2283–2291 (2004).
36. F. T. S. Yu and E. Y. Wang, "Speckle reduction in holography by means of random spatial sampling," *Appl. Opt.* **12**(7), 1656–1659 (1973).
37. V. Bianco, M. Paturzo, P. Memmolo, A. Finizio, P. Ferraro, and B. Javidi, "Random resampling masks: a non-Bayesian one-shot strategy for noise reduction in digital holography," *Opt. Lett.* **38**(5), 619–621 (2013).
38. V. Micó, C. Ferreira, and J. García, "Surpassing digital holography limits by lensless object scanning holography," *Opt. Express* **20**(9), 9382–9395 (2012).
39. Z. Wang and A. C. Bovik, "A universal image quality index," *IEEE Signal Process. Lett.* **9**(3), 81–84 (2002).
40. P. Memmolo, C. Distante, M. Paturzo, A. Finizio, P. Ferraro, and B. Javidi, "Automatic focusing in digital holography and its application to stretched holograms," *Opt. Lett.* **36**(10), 1945–1947 (2011).

1. Introduction

In recent years, DH [1–3] has led to the development of many spectacular applications, such as microscopic imaging and phase-contrast digital holographic microscopy, optical manipulation and characterization of living cells [4,5] and 3D holographic display [6]. In visible range holograms are digitally recorded by CCD or CMOS matrix sensors, while with IR laser source are detected by micro-bolometer array [7]. Holographic reconstruction can be performed either numerically or optically through a Spatial Light Modulator (SLM) [8–11]. However, due to the coherent nature of the emitting source, digital holograms may be degraded by the presence of both multiplicative speckle and incoherent additive noise [12], whose mixture is very hard to model statistically. On the other hand, speckle noise is useful for biomedical diagnosis [13]. Nevertheless, for display applications, classic filter based methods [14–16] have been extensively studied, but they can be applied only to the amplitude reconstruction, producing an improved visualization. So far, very few one-shot digital filtering based methods have been proposed which also provide a synthetic denoised hologram, suitable to be used in a 3D display [17,18]. Other kinds of denoising strategies rely on optical arrangements and they are basically divided into two classes. The first one consists in engineering the laser source, thus reducing its coherence [19–22]. The second class of methods is based on the introduction of some kind of “speckle diversity” between multiple acquisitions, which provides different speckle patterns, and produces a series of uncorrelated noisy holograms [23–33]. Uncorrelation between the holograms during the acquisition step is usually obtained by changing polarization [29], wavelength [30], or time diversity by means of moving diffusers [23,24], or even a turbid media changing the propagation conditions [31–33]. A suitable combination of numerical reconstructions of multiple holograms, typically by a multiplexing procedure, allows achieving a noise reduction. The majority of multiplexing approaches are based on a straightforward Average Sum (AS). A special case is represented by the optical scanning holography technique, whose incoherent mode makes it possible to record a complex hologram without noise [34]. The latter could be digitally converted into an off-axis real hologram and reconstructed by using a SLM. However, in these cases a complex ad hoc experimental set-up is required and the acquisition time unavoidably increases. On the other hand, one-shot techniques work on one single image acquisition and apply numerical filtering for reducing the noise on the corresponding DH reconstruction, but at the cost of a deterministic resolution loss [16,35]. A possible strategy to solve this trade-off is the numerical simulation of noise variation on a single digital hologram creating multiple uncorrelated reconstructions by a stack of random resampling masks, which are applied to the recorded hologram [36,37]. On the other hand, great effort has been spent to overcome the optical resolution limit in DH and the most common and effective techniques rely on scanning systems for recording holograms where each one carries information associated to different spatial frequencies of the object. These holograms are properly combined in a suitable domain to achieve a super-resolved reconstruction of the object [35–38]. In particular, in [38] Lensless Object Scanning Holography (LOSH) has been demonstrated to be a reliable technique to achieve at the same time super-resolution, field of view enlargement and noise reduction, thus showing fascinating perspectives for overcoming the DH constraints. However, multiple holograms based strategy allows a denoised visualization only in numerical reconstruction (either of the amplitude and phase) but it does not give the opportunity to directly synthesize a new digital hologram in order to reduce the speckle noise in the optical projection of digital holograms by SLM. To the best of our knowledge, no technique has been proposed before which is able to directly obtain such an appropriate hologram, thus severely limiting the quality of DH projections. Here we propose an encoding method for directly combining multiple digital holograms, with the aim to achieve image improvement in numerical as well as in optical reconstruction. It is worth to notice that our method is suitable for all kind of objects for which AS is required and the corresponding

synthetic hologram is needed. We apply it in the proper holograms synthesis for speckle-noise reduction in optical display applications. We numerically compare our synthetic complex wavefront with the AS and we also perform a test by projecting the hologram with a SLM, thus demonstrating the feasibility and the accuracy of the proposed method.

2. Mathematical formulation

The proposed strategy is structured in two main steps. The first one consists of finding an approximation of the AS that can be manipulated to synthesize a single hologram, while the second step is related to the synthesis procedure. We start from a generalization of the binomial formula, that permits to express the N th power of the sum of N elements. In our case we express the N th power of AS of amplitude reconstructions as

$$\mathbf{A}^N = \frac{1}{N^N} \sum_D \frac{N!}{l_1! \dots l_N!} \prod_{i=1}^N \mathbf{A}_i^{l_i}, \quad (1)$$

where we used a bold notation for matrices. In Eq. (1) $D = \{0 \leq l_1, \dots, l_N \leq N : \sum_i l_i = N\}$, $\mathbf{A} = 1/N \sum_i \mathbf{A}_i$ is the AS in which $\mathbf{A}_i = |\mathbf{C}_i|$, for $i = 1, \dots, N$, are the amplitude reconstructions of the N recorded holograms, \mathbf{H}_i , of the same object in the in-focus plane, obtained numerically by computing the diffraction Fresnel propagation integral. The latter is related to the Fourier transform by the following equation:

$$\mathbf{C}_i = \mathbf{Z} FT\{\mathbf{H}_i \mathbf{W}\} \quad (2)$$

where $FT\{\bullet\}$ is the Fourier transform and we define:

$$\mathbf{Z} = \left\{ z_{x,y} = \frac{\exp(j2\pi d/\lambda)}{j\lambda d} \exp(j\pi(x^2 + y^2)/\lambda d) \right\} \quad (3)$$

$$\mathbf{W} = \left\{ w_{k,q} = \exp\left(j\frac{\pi}{\lambda d}(k^2 p_x^2 + q^2 p_y^2)\right) \right\}$$

In Eq. (2), λ is the laser wavelength, d is the focus reconstruction distance and (p_x, p_y) are the pixel sizes in the hologram plane. We observe that, in the summation of Eq. (1), the only term which is obtained by the combination of all of the N amplitude reconstructions is given for $l_1 = l_2 = \dots = l_N = 1$. Neglecting the other contributions, we demonstrate that an effective multiplexing formula is given by

$$\mathbf{A} \approx \frac{1}{N} \left(N! \prod_{i=1}^N \mathbf{A}_i \right)^{\frac{1}{N}} \quad (4)$$

Obviously, this approximation would be correct only if all neglected terms were approximately zero. However, the equivalence in Eq. (4) is understood as a comparison of two different encoding ways. Hence, we look at their comparison in terms of visualization improvement. In order to clarify and demonstrate the validity of the Eq. (4), we will evaluate the performance of these encoding strategies by calculating the universal image quality index (UIQI) [39], which is designed to quantify any distortion between two images. However, the most remarkable feature of the adopted approach lies in the possibility to rewrite the term on the right hand side of Eq. (2) in a form which allows to synthesize a denoised hologram. In fact, by substituting Eq. (2) in Eq. (4) and neglecting the multiplicative constant contribution, we rewrite Eq. (4) as follow:

$$\begin{aligned} \left(\prod_{i=1}^N \mathbf{A}_i \right)^{\frac{1}{N}} &= \left| \mathbf{Z}^N \prod_{i=1}^N FT \{ \mathbf{H}_i \mathbf{W} \} \right|^{\frac{1}{N}} = \left| \mathbf{Z}^N FT \{ \mathbf{H}_1 \mathbf{W} * \mathbf{H}_2 \mathbf{W} * \dots * \mathbf{H}_N \mathbf{W} \} \right|^{\frac{1}{N}} = \\ &= \left| \mathbf{Z} FT_{[0,1]} \{ \mathbf{H}_1 \mathbf{W} * \mathbf{H}_2 \mathbf{W} * \dots * \mathbf{H}_N \mathbf{W} \} \right|^{\frac{1}{N}} = \left| \mathbf{C}_{synth} \right| \end{aligned} \quad (5)$$

The second equality in Eq. (5) is obtained by using the convolution theorem (“*” is the convolution operator) and the third equality is obtained by normalization of the amplitude of the Fourier transform in the range [0,1]. Notice that, in the last term we define \mathbf{C}_{synth} as the synthetic complex wavefront obtained from initial reconstructions by using the multiplexing formula in Eq. (4). Finally, the proposed encoding formula is obtained by back-propagation of \mathbf{C}_{synth} in the hologram plane

$$\mathbf{H}_{synth} = \mathbf{Z}_{BP} FT \{ \mathbf{C}_{synth} \mathbf{W}_{BP} \} \quad (6)$$

where \mathbf{Z}_{BP} and \mathbf{W}_{BP} are the same of Eq. (3), but using the opposite sign of the reconstruction distance and the pixel sizes in the image plane.

3. Experimental setups for hologram recording and holographic display

The holograms were recorded in a lens-less configuration as sketched in the Fig. 1(a). The light source is a 532 nm, Diode-Pumped Solid State laser, whose beam, after being spatially filtered and expanded by a collimator (C), is split by a beam-splitter cube (BS). The transmitted beam impinges on a ground-glass (G), attached to a rotator, at a distance of 35 cm from the object. The light scattered by the ground glass is used to illuminate the object (O). The beam that is reflected by the BS impinges on the camera sensor, through a couple of mirrors (M), and acts as reference-beam. The holograms were recorded by a CCD camera, with a resolution of 1280x1024 (6.7 micrometers square pixels), at a distance of 85 cm from the object. For each object, a sequence of holograms was recorded, by rotating the ground glass by five degrees steps. The optical reconstruction of the holograms has been achieved by use of a Spatial Light Modulator (SLM) as shown in Fig. 1(b). The hologram was displayed by the SLM which was a phase-only SLM-LCOS (PLUTO-by Holoeye, $8\mu\text{m}$ pixel pitch), irradiated by a polarized and collimated laser beam at wavelength $\lambda = 532\text{nm}$. The reconstructed wavefront was focused on a CCD sensor by a converging lens (L) with focal length $f = 40$ mm, for obtaining the final image. We consider an astronaut puppet as a test object in our experiments (see Fig. 1(c) for its photograph).

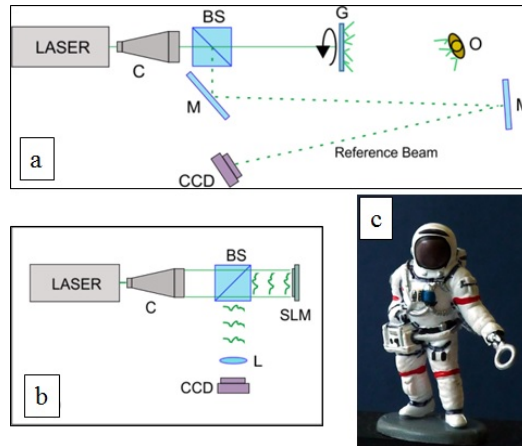


Fig. 1. setups for holograms recording (a) and optical display (b). In (c) a photograph of the object used in the experiments.

4. Results and discussions

We test the proposed method in two different scenarios. First, we acquire two sequences of 7 uncorrelated digital holograms of an astronaut puppet with time diversity obtained using a moving diffuser. In particular, we record two different speckle patterns characterized by both thin speckle and large speckle grains. For both experimental sequences, we calculate the two multiplexed reconstructions reported in Eq. (4), i.e. the AS method and the method proposed in this paper. Our aim is to demonstrate the validity of Eq. (4) by quantifying how the AS is well-approximated by the proposed multiplexing method. For this purpose, we use UIQI as a performance parameter, which is defined as [39]

$$\text{UIQI} = \frac{\text{cov}(O,P)}{\sigma(O)\sigma(P)} \cdot \frac{2\mu(O)\mu(P)}{\mu^2(O)+\mu^2(P)} \cdot \frac{2\sigma(O)\sigma(P)}{\sigma^2(O)+\sigma^2(P)} \quad (7)$$

where $\sigma(\bullet)$, $\mu(\bullet)$ and $\text{cov}(\bullet,\bullet)$ are the standard deviation, the average value and the covariance operators, respectively. UIQI gives a percentage of similarity between two images. The first component calculates the correlation coefficient between the AS, “ O ”, and the result of the proposed strategy, “ P ”. It measures the degree of linear correlation between the two images. The second factor measures the closeness of the mean luminance between the images; and the last term measures the similarity between the contrast of the two images, because the standard deviation is a contrast index. Therefore, the last two components take into account the relative distortions between the images [39]. In Fig. 2 we report the results of the two multiplexing strategies.

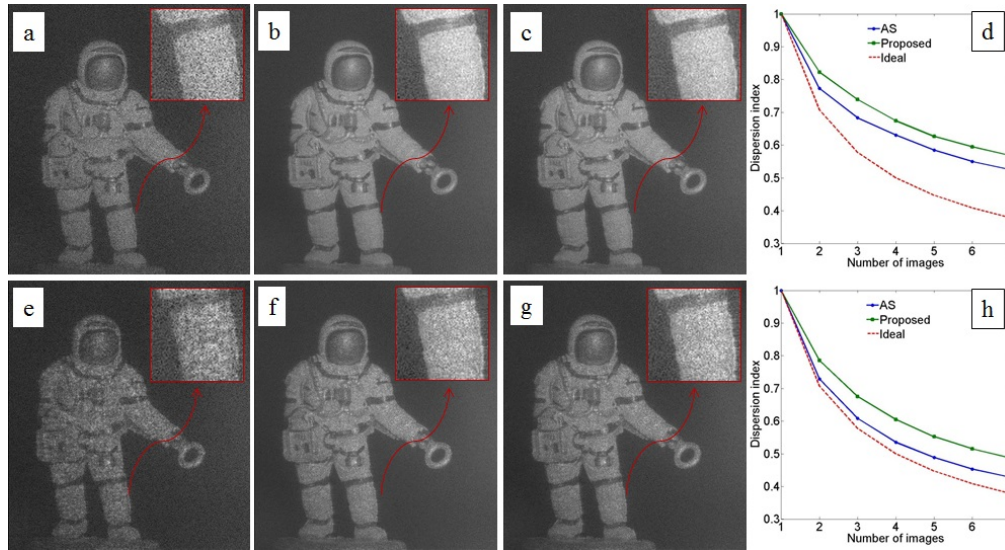


Fig. 2. Thin speckle (top row) and large speckle (bottom row) cases. (a,e) are the numerical reconstructions of one of recorded holograms with thin and large speckle grains respectively. (b,f) are the results of AS method, while (c,g) are the results obtained by using the proposed method. (d,h) DI vs. the number of images in case of thin (d) and large (h) speckle grains. DI is normalized with respect to the DI obtainable with one single reconstruction. Green solid line: proposed method. Blue solid line: AS method. Red dashed line: DI in case of uncorrelated images (ideal trend).

In particular, we show one of the seven holograms recorded with thin (Fig. 2(a)) and large (Fig. 2(e)) speckle grains, while the other sub-figures show the results of AS (Fig. 2(b) and Fig. 2(f)) and the proposed method (Fig. 2(c) and Fig. 2(g)). In all figures, an inset shows details of the astronaut leg. A remarkable speckle reduction with respect to the unprocessed images (i.e. the reconstructions of one single hologram) is apparent in the reconstructions

obtained both with the AS and the proposed method. By preliminary comparison between the two strategies, we do not observe significant differences, as it is also confirmed by the calculation of UIQI, which results 99% and 98% for the thin and large speckle cases, respectively. As a quantitative performance measure, we evaluated the Dispersion Index (DI) defined as [33]

$$DI = \sigma(I) / \mu(I) \quad (8)$$

where I is the image. Since this is measured over a homogeneous segment of the image, i.e. where a smooth behavior of the gray levels is expected, any fluctuation around the mean value has to be attributed to the noise, so that noise reduction results in a lowering of DI. In Fig. 2(d) and Fig. 2(h) are shown the trend of the DI obtained by increasing the number of combined holograms, in cases of thin and large speckle grains, respectively. In particular, the blue and the green solid lines respectively show that the dispersion reduction is achieved by adopting the AS and the proposed method. With the red dashed line, the boundary curve trend is observed, i.e. the trend obtained by averaging uncorrelated speckle patterns. As expected, a significant dispersion reduction is obtained with both methods, as the measured gain is higher than 40% in the case of thin speckle and higher than 50% in case of large speckle grains. A similar trend is shown by the plots of the AS and the proposed method which has the remarkable advantage of being applicable to the holographic optical displays. These results demonstrate that Eq. (4) is correct, i.e. the proposed multiplexing method is a reliable candidate to substitute the AS method. Therefore, by using Eq. (5) and Eq. (6), we can synthesize a proper hologram without losing the gained enhancement. Hence, we perform the optical display of synthesized holograms, retrieved by Fig. 2(c) and Fig. 2(g), comparing them with the optical reconstructions of one of the recorded holograms. These results are reported in Fig. 3.

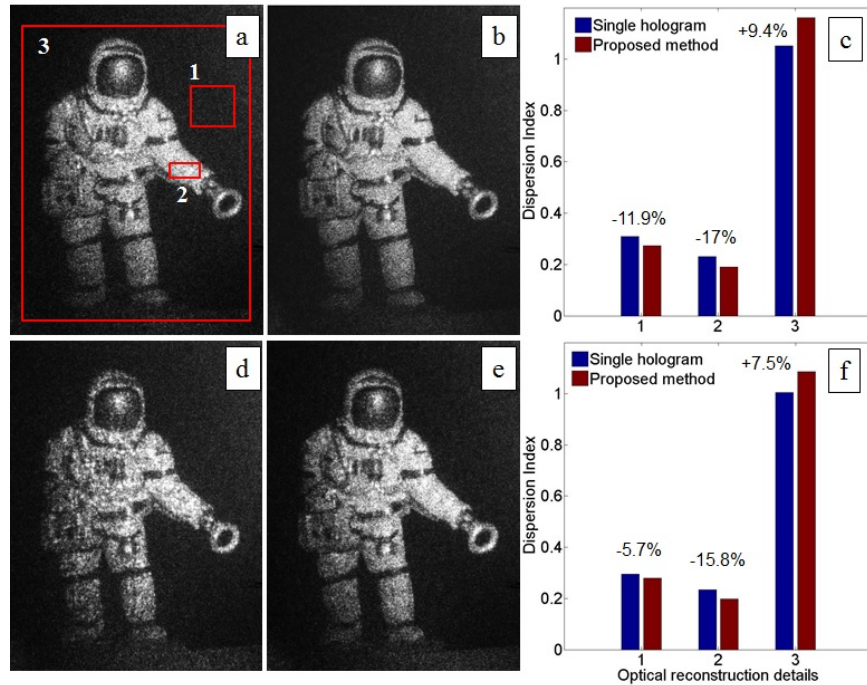


Fig. 3. Optical reconstruction of astronaut puppet with original thin (a) and large (d) speckle grains. In (b,e) we show the optical display of the corresponding synthesized holograms obtained by using the encoding formula in Eq. (6). (c,f) DI measured over the image segments indicated by the red boxes in Fig. 3(a), in case of thin (c) and large (f) speckle.

Optical projections show that the encoding formula allows for reconstructions with highly reduced noise in both cases. In particular, in Fig. 3(a) and Fig. 3(d) the optical projections of initial holograms of astronaut puppet with thin and large speckle grains respectively, are reported, while in the denoised optical reconstructions of Fig. 3(b) and Fig. 3(e) speckle reduction results in a smoother trend of the gray level distribution in the homogeneous area of the image and the background, and a contrast enhancement on the edges. In order to quantify the improvement, we selected three significant areas in the images of Fig. 3 where DI measures are obtained (see the red boxes in Fig. 3(a)). In Fig. 3(c) and Fig. 3(f) are shown the DI obtained in the three areas in case of thin and large speckle grains, respectively. In particular, the bar plot shows a significant DI reduction with respect to the single hologram projection in the background and the homogeneous object segment (e.g. 11,9% reduction in the area “1”, and 17% reduction in the area “2” in case of thin speckle). In order to quantify the contrast enhancement, the DI has been measured on the area “3” including the whole object. Indeed, in [40] it has been shown that the approximation of Tamura coefficient (i.e. the square root of the DI defined as in [33]) can be used to measure the image contrast, as image de-focusing and/or speckle-noise provoke its reduction. Hence, image contrast enhancement in turn results in increasing the Tamura coefficient. Noteworthy, adopting the proposed method, we found a 9,4% improvement of the optical reconstruction in case of thin speckle, while we measured a 7,5% contrast enhancement in case of large speckle grains.

5. Conclusion

In this work, a new hologram encoding strategy has been introduced which allows to directly synthesize in a single complex wavefront the contribution of multiple acquisitions. In this way, the proposed method is able to improve both the numerical and the optical reconstructions. If the recordings are performed in order to provide speckle diversity, a denoised projection is achievable. Experiments have been carried out to validate the method effectiveness, and to compare its performance with the commonly used AS. Results have shown a remarkable noise suppression with respect to the processing of a single hologram. We found comparable results between the AS and the proposed method, but the latter possesses the intrinsic advantage to be suitable for optical projection and 3D display purposes. The gain in terms of speckle reduction and contrast enhancement has been quantitatively evaluated both on the numerical and the optical reconstructions.

Acknowledgments

We are very grateful to Dr. Andrea Finizio of CNR-Istituto Nazionale di Ottica of Napoli to have acquired the holograms of astronaut and for his constructive feedback and careful reading of the paper. This research was funded by the MIUR (Italian Ministry for Research and University) within the PON project IT@CHA PON01_00980 Italian Technologies for Advanced Application in Cultural Heritage Assets.